Mössbauer spectroscopic study of low-frequency vibrational modes in sintered metal powders

M. Hayashi,* E. Gerkema,† and A. M. van der Kraan

Interfacultair Reactor Instituut, Delft University of Technology, 2629 JB Delft, The Netherlands

I. Tamura

Physics Department, Toyama Medical and Pharmaceutical University, Toyama 930-01, Japan

Low-frequency vibrational modes in sintered copper and silver powders have been studied by [197]Au Mössbauer spectroscopy. A decrease in resonance absorption area has been found for the sinters compared with the values found for bulk materials. In the spectra of a copper sinter of low packing fracton (26.7%), a broad spectral component was clearly observed, superimposed on the normal Mössbauer line. This broad line is interpreted to arise from low-frequency modes due to oscillations of the particles in the sinters. The temperature dependence of the Mössbauer absorption area can be explained by a model based on dispersion theory combined with the Debye model and the fracton model used for describing phonons in a particle and particle oscillations in a sinter, respectively. The energies of the low-frequency modes determined from the Mössbauer measurements range from ≈ 2 mK to several hundred millikelvin (in equivalent temperature) and coincide within a factor of 6 with the values estimated from ultrasonic data [M. C. Maliepaard et al., Phys. Rev. B 32, 6261 (1985)] using the fracton model, providing support for the localized nature of the modes.

I. INTRODUCTION

The origin of the anomalous thermal boundary (Kapitza) resistance between liquid helium and sintered metal heat exchangers in the millikelvin temperature range had been a puzzle for a long time after this phenomenon was observed by Avenel et al.[1] in 1973. Now it is generally believed that low-frequency vibrational modes in the sinters are responsible for the anomalous thermal resistance. These modes are mainly related to the oscillation of the particles in a sinter caused by the restoring forces exerted through the bridges connecting the sinter particles.

Since the importance of the low-frequency modes was suggested by Frisken et al.[2] in 1981, there has been a number of theoretical studies aimed at explaining the anomalous heat transfer between liquid helium and the sintered metal powder in terms of the vibrational modes. Nishiguchi and Nakayama[3] demonstrated, by approximating the low-frequency modes by Einstein oscillators and calculating the heat transfer between zero sound in liquid ^{3}He and the low-energy modes, that experimental data on sintered silver particles of 1 μm diameter[4] can be quantitatively explained by adjusting the parameters appearing in the theory. Rutherford et al.[5] calculated the heat transfer between the low-energy modes and liquid helium in the pores of the sinters by means of a "shaking box" model, in which each pore was treated as an oscillating cubic box containing ^{3}He quasiparticles. The resulting heat transfer was found to be within a factor of 2 or 3 of experimental data while the temperature dependence was correct.

However, there are only a few experimental works that support the existence of such low-energy modes. Recently, thermal properties of random systems including sin-

tered metal powder have attracted much interest. The concept of fractals has been applied to the vibrational properties of such systems, and a "fracton" model was proposed.[6,7] According to this model, very low-frequency vibrations can propagate in the system like a phonon in continuous medium, but there is crossover frequency beyond which the vibrational modes are localized (fracton). According to Rutherford et al.,[5] for sintered submicrometer metal powder, the frequency range of the localized modes includes the frequencies which are most effective for the heat transfer between liquid helium and the sinter below a temperature of 10 mK. Maliepaard et al.[8] measured the attenuation of ultrasonic waves in the MHz range passing through discs of sintered copper poweder particles of 10 μm average diameter as a function of frequency. They found that there exists a band edge at a phonon wavelength of about ten times the particle diameter, beyond which sound does not propagate. This observation indicates a crossover from low-frequency propagating phonons to localized modes of higher frequencies, providing indirect support for the existence of localized modes.

It has been shown both theoretically and experimentally[9−12] that, in Mössbauer spectroscopy, the vibration of particles in a system of interacting small particles causes a reduction of the observed recoilless fraction. For particles with a diameter over several nm, the probability of phonon excitations in each particle during the γ absorption is the same as in the bulk material. The excitation of a particle oscillation in the system will cause an additional reduction of the recoilless fraction. Hayashi et al.[13] studied by [197]Au Mössbauer spectroscopy sintered particles of gold and of copper-gold alloy of 50 nm average diameter. They found a systematic increase in linewidth with decreasing packing fraction (occupied volume frac-

tion) of the sinters. The increase in linewidth was attributed to the particle oscillation in the sinters; the absorption accompanied by the excitation of the low-frequency modes gives rise to a broad line which overlaps the recoilless Mössbauer line, making the latter apparently broader. The measurements, however, have been made at only one temperature, 16 K. Moreover, the alloy particles did have a poor homogeneity in composition; they consisted of roughly two components, one Cu-rich and one Au-rich. The experimental results have been interpreted on the basis of a classical theory, which is semi-quantitative and contains defects due to neglecting quantum effects. These facts may cast some doubt on the correctness of the conclusion drawn.

The purpose of this paper is to extend the study of Ref. 13 in order to obtain more accurate information. Therefore, in the present work, the homogeneities of the alloy particles are improved, the Mössbauer effect is measured as a function of temperature for sinters as well as for foils, and the discussion will be based on a much more accurate quantum theory.

II. THEORY

In this section, a quantum-theoretical formula for the absorption spectrum of dense packed or sintered small particles will be derived. The details of the derivation will be described elsewhere. According to the dispersion theory, the cross section of absorption of a γ ray of energy E by a single nucleus in a system of interacting atoms is given by

$$\sigma_a(E) = \frac{\sigma_0 \Gamma_0^2}{4} \sum_{n,n_0} g_{n_0} \frac{|\langle n | \exp(i\mathbf{p}\cdot\mathbf{r}/\hbar)|n_0\rangle|^2}{(E_0 - E + \varepsilon_n - \varepsilon_{n_0})^2 + \Gamma_0^2/4} , \quad (1)$$

where $\mathbf{p}$ is the momentum of the γ ray, $\mathbf{r}$ the coordinate of the nucleus, and E_0 the energy difference between the final and the initial nuclear state. ε_n and ε_{n_0} are the energies of states $|n\rangle$ and $|n_0\rangle$ of the interacting system, respectively, Γ_0 is the natural width of the excited state of the nucleus, g_{n_0} is the statistical weight factor for the state $|n_0\rangle$, and σ_0 is the resonance absorption cross section.

Using the time-dependent correlation function method developed by van Hove,[14] Singwi and Sjölander[15] have shown that for monatomic crystals of cubic symmetry Eq. (1) can be written as

$$\sigma_a(E) = \frac{\sigma_0 \Gamma_0}{4\hbar} \int_{-\infty}^{\infty} \exp\left[-\frac{it}{\hbar}(E - E_0) - \frac{\Gamma_0}{2\hbar}|t|\right]$$
$$\times \exp[-\tfrac{1}{2}\kappa^2 \gamma_a(t)]dt , \quad (2)$$

where $\gamma_a(t)$ represents a correlation between the displacements of the atom from the equilibrium point at two different times separated by t and is given by

$$\gamma_a(t) = \frac{\hbar^2}{m_0} \int_0^{\infty} \left\{\coth\left[\frac{z}{2k_B T_a}\right]\left[1 - \cos\left[\frac{zt}{\hbar}\right]\right]\right.$$
$$\left. - i \sin\left[\frac{zt}{\hbar}\right]\right\} \frac{\phi_a(z)}{z}dz . \quad (3)$$

In Eqs. (2) and (3), $\hbar\kappa = p$, m_0 is the mass of an atom, T_a is the temperature of the absorber, and $\phi_a(z)$ is the distribution of energy levels of the phonons normalized such that $\int_0^{\infty} \phi_a(z)dz = 1$ and $\phi_a(z)$ is zero beyond $z = z_{max}^{ph}$.

For a system in which small particles (microcrystals) are packed or sintered, the displacement of the nucleus from the equilibrium point is due to both lattice phonon (ph) and particle oscillation (PO). If it is assumed that ph and PO are independent of each other, $\gamma_a(t)$ can be expressed as a sum of two independent parts:

$$\gamma_a(t) = \gamma_a^{ph}(t) + \gamma_a^{PO}(t) . \quad (4)$$

In Eq. (4), $\gamma_a^{ph}(t)$ is given by the right-hand side of Eq. (3) while $\gamma_a^{PO}(t)$ is given by the same equation with m_0 changed into M_0, the mass of a particle, and $\phi_a(z)$ changed into $\Phi(z)$, which is the energy level distribution of PO in such a way that $\int_0^{\infty} \Phi(z)dz = 1$ and $\Phi(z) = 0$ for $z > z_{max}^{PO}$.

Dividing the range of integration $(-\infty, \infty)$ in Eq. (2) into a number of subranges, and adopting approximations of $\gamma_a^{ph}(t)$ and $\gamma_a^{PO}(t)$ in each subrange, a physically more comprehensible formula for the absorption cross section is obtained:

$$\sigma_a(E) = \frac{\sigma_0 \Gamma_0^2}{4}\exp(-2W_a^{ph})\exp(-2W_a^{PO})\frac{1}{(E-E_0)^2 + (\Gamma_0/2)^2}$$
$$+ \frac{\pi^{1/2}\sigma_0\Gamma_0}{2\Delta}\exp(-2W_a^{ph})[1-\exp(-2W_a^{PO})]\exp\left[-\frac{(E-E_0-P)^2}{\Delta^2}\right]$$
$$+ \frac{\pi^{1/2}\sigma_0\Gamma_0}{2(\delta_a^2 + \Delta^2)^{1/2}}[1-\exp(-2W_a^{ph})]\exp\left[-\frac{(E-E_0-R-P)^2}{\delta_a^2 + \Delta^2}\right] , \quad (5)$$

where $R = \hbar^2\kappa^2/2m_0 = E_0^2/2m_0 c^2$ (recoil energy of a free nucleus), $P = \hbar^2\kappa^2/2M_0 = E_0^2/2M_0 c^2$ (recoil energy of a free particle),

$$\delta_a^2 = 2R \int_0^{\infty} z \coth\left[\frac{z}{2k_B T_a}\right]\phi_a(z)dz , \quad (6)$$

$$\Delta^2 = 2P \int_0^{\infty} z \coth\left[\frac{z}{2k_B T_a}\right]\Phi(z)dz , \quad (7)$$

$$2W_a^{ph} = \tfrac{1}{2}\kappa^2\gamma_a^{ph}(\infty) = R \int_0^{\infty} \frac{\phi_a(z)}{z}\coth\left[\frac{z}{2k_B T_a}\right]dz , \quad (8)$$

and

$$2W_a^{PO} = \frac{1}{2}\kappa^2\gamma_a^{PO}(\infty) = P\int_0^\infty \frac{\Phi(z)}{z}\coth\left[\frac{z}{2k_BT_a}\right]dz . \quad (9)$$

In Eq. (5), the first term represents the Mössbauer line, the second term comes from the absorption with simultaneous excitation of PO (PO band) and the third term consists of the absorption accompanied by phonon excitation (phonon wing). The two components making up the phonon wing, one with and the other without PO excitation, are practically inseparable. Equation (5) shows that the Mössbauer line is an upshifted Lorentzian of width [full width at half maximum (FWHM)] Γ_0, the PO band is a Gaussian having a width (FWHM) $2(\ln 2)^{1/2}\Delta$ and shifted by P, and the phonon wing is a Gaussian of width $2[\ln 2(\delta_a^2 + \Delta^2)]^{1/2}$, which is shifted by $R + P$. It should be noted that because of the largeness of δ_a the phonon wing merges in the background while the PO band may or may not be observed in the spectrum. The integrated intensities of the three components are equal to $\frac{1}{2}\pi\sigma_0\Gamma_0 f_a F_a$, $\frac{1}{2}\pi\sigma_0\Gamma_0 f_a(1 - F_a)$, and $\frac{1}{2}\pi\sigma_0\Gamma_0(1 - f_a)$ $\{ = \frac{1}{2}\pi\sigma_0\Gamma_0[(1 - f_a)F_a + (1 - f_a)(1 - F_a)]\}$, respectively, where $f_a = \exp(-2W_a^{ph})$ is the recoilless fraction due to

the lattice phonons and $F_a = \exp(-2W_a^{PO})$ is the recoilless fraction due to PO. The sum of the integrated intensities over the three components equals $\frac{1}{2}\pi\sigma_0\Gamma_0$, in agreement with the requirement that the integrated intensity of a spectrum must always equal $\frac{1}{2}\pi\sigma_0\Gamma_0$. The factor $\frac{1}{2}\pi\sigma_0\Gamma_0$ is the result of our choice of σ_0 such that $\sigma_a(E_0) = \sigma_0$.

In Mössbauer spectroscopy one is experimentally dealing with the self-absorption cross section $\sigma(s)$ which for a thin absorber is defined by

$$\sigma(s) = \int_0^\infty \sigma_a(s + E)w_e(E)dE / \int_0^\infty w_e(E)dE$$
$$= \int_0^\infty \sigma_a(s + E)w_e(E)dE , \quad (10)$$

where $s = (v/c)E_0$ is the energy Doppler shift caused by moving the emitter with velocity v relative to the absorber. The probability $w_e(E)$ for the emission of a γ ray is given by Eq. (1) except that the signs of ε_n and ε_{n_0} are interchanged and $w_e(E)$ is normalized such that $\int_0^\infty w_e(E)dE = 1$. Following Singwi and Sjölander's method[15] as before, the following approximate formula can be obtained:

$$\sigma(s) = \frac{\sigma_0\Gamma_0(\Gamma_0 + \Gamma_e)}{4}\exp(-2W_e - 2W_a^{ph} - 2W_a^{PO})\frac{1}{s^2 + (\Gamma_0 + \Gamma_e)^2/4}$$

$$+ \frac{\pi^{1/2}\sigma_0\Gamma_0}{2\Delta}\exp(-2W_e - 2W_a^{ph})[1 - \exp(-2W_a^{PO})]\exp\left[-\frac{(s - P)^2}{\Delta^2}\right]$$

$$+ \frac{\pi^{1/2}\sigma_0\Gamma_0}{2(\delta_e^2 + \delta_a^2 + \Delta^2)^{1/2}}[1 - \exp(-2W_e - 2W_a^{ph})]\exp\left[-\frac{(s - 2R - P)^2}{\delta_e^2 + \delta_a^2 + \Delta^2}\right] \quad (11)$$

with

$$\delta_e^2 = 2R\int_0^\infty z\coth\left[\frac{z}{2k_BT_e}\right]\phi_e(z)dz \quad (12)$$

and

$$2W_e = \frac{1}{2}\kappa^2\gamma_e(\infty) = R\int_0^\infty \frac{\phi_e(z)}{z}\coth\left[\frac{z}{2k_BT_e}\right]dz . \quad (13)$$

Here T_e is the temperature of the emitter and $\phi_e(z)$ is the normalized energy spectrum of the phonons in the emitter and $\phi_e(z)$ vanishes beyond $z = z_{max}^e$. In Eq. (11), source line broadening is taken into account by introducing Γ_e instead of Γ_0.

By comparing Eq. (11) with Eq. (5), it can be seen that in an experimentally obtained spectrum $\sigma(s)$ the width of the Mössbauer line is approximately doubled (increased by Γ_e) as compared to that in the absorption cross-section spectrum $\sigma_a(E)$, while the width of the PO band is not changed and the width of the phonon wing is increased by a factor of about $2^{1/2}$. The comparison also shows that the shift of the PO band is not changed while the shift is approximately doubled (increases by R) for the phonon wing.

III. EXPERIMENT

The alloy particles were produced by first melting the mixtures of the constituent metals in an arc in Ar gas of 1 atm into the alloys, and then evaporating the alloys in low-pressure Ar gas (1 Torr for Ag-Au and 5 Torr for Cu-Au) as described in Ref. 13. The metals had purities 99.99% (Au and Ag) and 99.9% (Cu). In order to improve the homogeneity in composition, only particles during the initial stage of the evaporation process were collected. Therefore the gold contents of the samples were much lower (Table I) than the 20 at. % of the original alloys. The Mössbauer spectra of the sinters consisted of a singlet with a linewidth nearly equal to the natural width, indicating a considerable improvement of the homogeneity. The particles were pressed into disks of 15 mm diameter and of various packing fractions using a die. After the pressing, the disks were sintered in vacuum at 493 K for 45 min. The specifications of the samples used in the present experiment are listed in Table I. The percentage of gold content of the sinters has been determined by instrumental neutron activation analysis method after the Mössbauer measurements. Afterwards, foils of equivalent compositions were produced and also

TABLE I. Specifications of samples.

Sample number	Composition	Au areal density ζ (mg/cm^2)	density n (cm^{-2})	Average particle diameter (nm)	Sintering condition	Packing fraction (%)	Sample weight (mg)	Sample diameter (mm)	Sample thickness (μm)
1		25.1	7.68×10^{19}			100 (foil)	400	14.5	
2	Cu–3.60 at.% Au	23.7	7.24×10^{19}		220 °C	54.3	393.6	14.8	470
3		24.0	7.34×10^{19}	150	45 min	26.7	403.2	14.9	965
4		24.1	7.37×10^{19}			≈ 2 (powder)	410	15.0	
5		13.0	3.99×10^{19}			100 (foil)	364	14.5	
6	Ag–3.33 at.% Au	13.0	3.97×10^{19}	50	220 °C	68.4	361.8	14.5	305
7		15.0	4.59×10^{19}		45 min	28.9	362.1	13.5	835

measured by Mössbauer spectroscopy. The average particle diameters of the prepared sinters were determined by inspecting the surfaces of the sinters by scanning electron microscopy.

The source was a 97.5%-enriched ^{196}Pt disk of 59 mg, irradiated for 24 h in a flux of 10^{12} neutrons/cm^2 sec. The source was installed in the spectrometer about 4 h after the end of the neutron irradiation and the activity of ^{197}Pt at that time was about 40 mCi. The source temperature was kept at 4.2 K throughout the experiments. Each fresh source was used for several days, during which time measurements on one sample were carried out at various temperatures. The 77.3-keV γ ray of ^{197}Au was measured with a germanium detector. Hence a large variation in the background intensity with time was not expected. In order to find out such a variation with time, the initial measurements were repeated, for the Cu-Au foil, with the same source after four days of the routine measurements and it was confirmed that there was no appreciable change in the intensity-to-background ratio during the four-day period. The measurements were performed in a sinusoidal mode, and the spectra were folded and linearized.

The radius of the γ-transmitting area of the sample holder was 14 mm, while the radius of the sample disks was 15 mm. Owing to the narrow margin on the periphery of the disks, the error caused by possible nonuniformity of packing fraction within the sample is minimized: If the transmitting area of the sample is considerably smaller than the entire area of the sample, nonuniformity may cause a difference in effective Au areal density for different samples, even if all samples contain the same amount of Au. (Even if the amount of Au in the transmitting area is the same, the recoilless fraction observed for a nonuniform sample will be smaller than for a perfectly uniform one. But this error will be small for a small effective absorber thickness.)

Because of the narrow margin and shrinkage of the samples during sintering (see Table I), there can be a narrow gap between the sample and the holder. Whenever there is such a gap, through which the γ ray can pass freely, this will cause an error in the observed background level. This problem will be taken up in Sec. IV.

Besides the sintered samples a powder sample of Cu-Au was prepared and measured for purposes of comparison. In the sample, the Cu-Au particles were very loosely packed without sintering and the particles had the same composition and size as the particles in the sinters (Table I).

IV. RESULTS AND DISCUSSION

In Fig. 1 spectra for the different Cu-Au samples measured at 60 K are shown with the least-squares-fitted Lorentzians assuming a flat background. The geometry of the apparatus assures that the background of the folded spectra is flat to a reasonable accuracy. Similar spectra have been obtained for the Ag-Au samples.

In Figs. 2(a) and 2(b) the temperature dependence of the absorption area per unit background normalized to the value at 4.2 K, $A_L(T)/A_L(4.2$ K), is plotted versus temperature T for the Cu-Au and Ag-Au samples. It is found that $A_L(T)/A_L(4.2$ K) decreases in the order of decreasing packing fraction for the Cu-Au samples, i.e., foil $> 54.3\%$ sinter $> 26.7\%$ sinter $>$ powder, indicating a reduction in recoilless fraction for the sinters and powder from the bulk value. Furthermore, the smaller the packing fraction and the higher the temperature, the
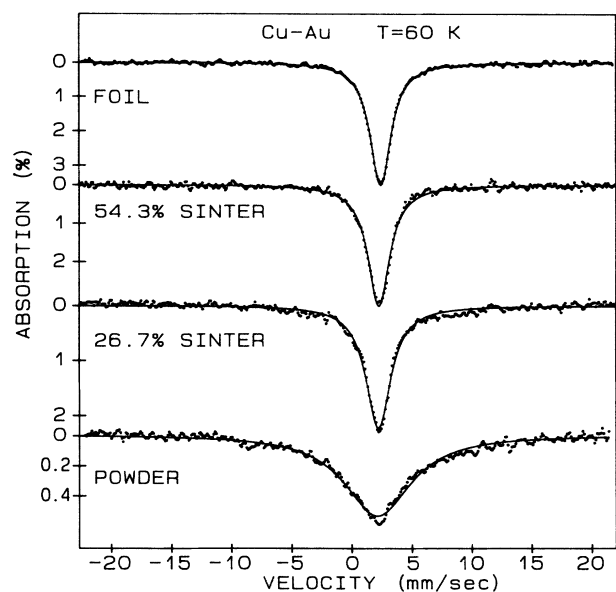

FIG. 1. Mössbauer spectra at 60 K of Cu-Au samples of different packing fractions with the least-squares-fitted Lorentzians.
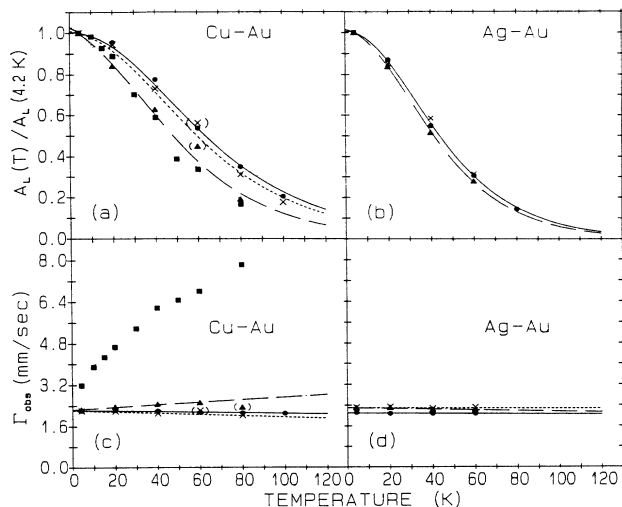
FIG. 2. Plot of the absorption area per unit background A_L determined by the Lorentzian fit and normalized to the value at 4.2 K and the plot of the determined linewidth Γ_{obs} as a function of temperature. (a), (c) for Cu-Au samples of different packing fractions. ●, foil; ×, 54.3% sinter; ▲, 26.7% sinter; ■, powder. (b), (d) for Ag-Au samples of different packing fractions. ●, foil; ×, 68.4% sinter; ▲, 28.9% sinter. The curves in (a) and (b) represent the calculated results based on a dispersion theoretical model fitted to the plotted data and the straight lines in (c) and (d) are the least-squares-fits to the data. The data points in parentheses were neglected in the fittings.

FIG. 3. Mössbauer spectra of a Cu-Au powder sample at different temperatures with the least-squares-fitted Lorentzians.

larger is the reduction. For Ag-Au samples, the effect is less remarkable. Only a small reduction is observed for the 28.9% sinter. As long as the geometry of the absorber-holder assembly does not change appreciably during the measurement of one sample with varying temperature, the values of $A_L(T)/A_L(4.2$ K) are correct even though the values of $A_L(T)$ may not be accurate on account of possible presence of a narrow gap between the sample and the holder as argued in Sec. III.

The linewidth (FWHM) Γ_{obs}, determined by the Lorentzian computer fit, is plotted versus T for all measured Cu-Au samples in Fig. 2(c) and for the Ag-Au samples in Fig. 2(d). For the Cu-Au powder and for the 26.7% Cu-Au sinter, Γ_{obs} increases with T. This result is consistent with the previous one by Hayashi et al.[13] For all other samples, however, Γ_{obs} remains constant or decreases slightly with increasing T.

By inspecting Fig. 1 carefully a discrepancy, although small, is found to exist between the experimental data and the fitted curves for the Cu-Au powder and 26.7% sinter samples. This discrepancy turns out to be systematic for these samples and becomes larger with increasing temperature as is shown in Fig. 3 for the Cu-Au powder sample. Both facts, the increasing Γ_{obs} and growing discrepancy between the experimental data and the fitted curves, indicate that a broad component is overlapping the Lorentzian line. According to the theoretical model described in Sec. II this additional component is ascribed to the PO band having approximately a Gauss-
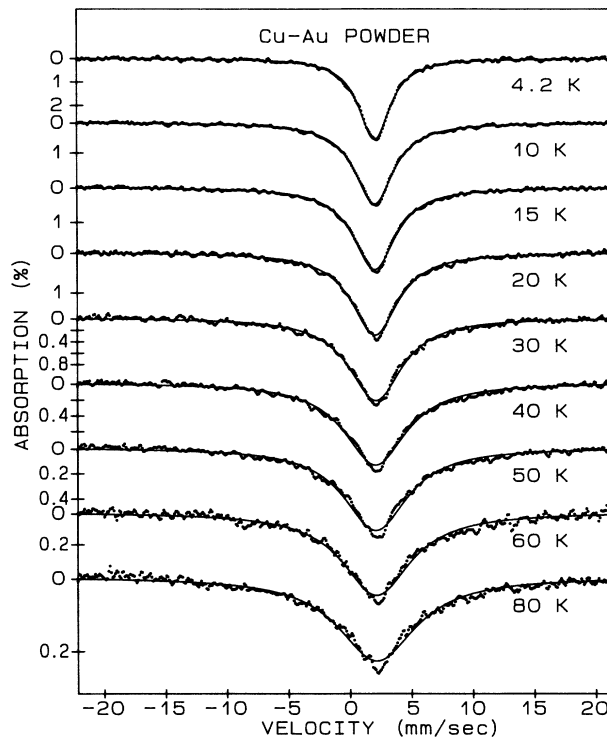
ian line shape. For the present particles, the expected shift P of the Gaussian line relative to the Lorentzian one is quite negligible. Fitting the spectra with a Lorentzian line and a Gaussian one, better fits are obtained, as is shown in Figs. 4(a) and 4(b) for the 26.7% Cu-Au sinter and Cu-Au powder, respectively. It turns out that the two-component fittings are unsuccessful for the 4.2 K spectrum of the 26.7% Cu-Au sinter and for all spectra of the other sinters; the depths of the Gaussians have become very small (typically by more than 2 orders of magnitude) compared to those of the corresponding Lorentzians and an accurate analysis will be impossible because of the statistical scatter in the spectra. In Fig. 5 the plot of $A_L(T)/A_L(4.2$ K) determined by the two-component fitting procedure is presented. In the figure the absorption area of the Gaussian line, A_G, normalized to $A_L(4.2$ K) of the Lorentzian one is also plotted. The determined widths Γ_{obs} of the Lorentzians and D_{obs} (FWHM) of the Gaussians are plotted versus T in Figs. 6 and 7. The width Γ_{obs} for the 26.7% Cu-Au sinter now coincides within the experimental error with those of the other Cu-Au sinters and the foil.

According to the approximate formula (11) [or (5)], the absorption area of the Mössbauer line varies as $f_a F_a$. Making use of this relation, the absolute values of the recoilless fractions f_a and F_a will be estimated. The recoilless fraction f_a for the gold atoms embedded in the alloys can be deduced from the data on the foils using the Debye model for $\phi_a(z)$, as this model has been proved to
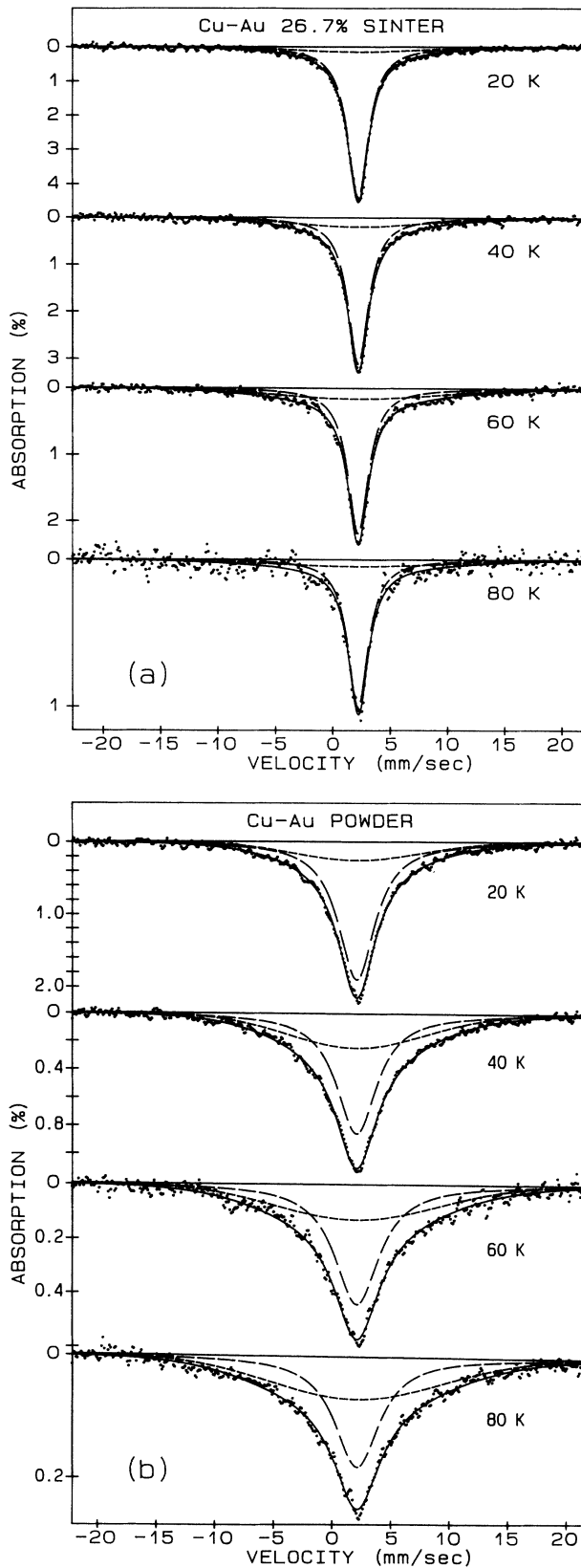
FIG. 4. Two-component (Lorentzian-plus-Gaussian) fitting of the Mössbauer spectra of (a) 26.7% Cu-Au sinter and (b) Cu-Au powder sample at different temperatures. ——, fitted absorption curve; ———, Lorentzian component; — — —, Gaussian component.

be a fairly good approximation in many cases of Mössbauer effect in bulk metals. The absorption area as a function of the effective absorber thickness, $S(t_a)$, has been conveniently tabulated in a table by Trooster and Viegers.[16] The effective absorber thickness t_a is defined as $t_a = \sigma_0 n f_a$, where n is the areal atomic density of Au. Hence the task is to fit

$$\frac{S(\sigma_0 n f_a(T))}{S(\sigma_0 n f_a(4.2 \text{ K}))} \tag{14}$$

to the experimental data of $A_L(T)/A_L(4.2 \text{ K})$. In expression (14), $S(t_a)$ can be approximated by a polynomial, σ_0 is equal to 3.86×10^{-20} cm^2, and the values of n are listed in Table I. So, the only free parameter left in the fit is the Debye temperature Θ. The deduced values of Θ for the Cu-Au and Ag-Au foils are tabulated in Table II. These values of Θ refer to the Au impurity atoms in the alloys and are considerably smaller than the values for pure Cu ($\Theta = 343$ K) or Ag ($\Theta = 225$ K) metals. The calculated curves for $A_L(T)/A_L(4.2 \text{ K})$ [$= S(\sigma_0 n f_a(T))/S(\sigma_0 n f_a(4.2 \text{ K}))$] using the Debye model and these values of Θ are represented by the solid lines in Figs. 2(b) and 5.

In order to determine the recoilless fraction F_a related to PO for the sinters and powder from the data of $A_L(T)/A_L(4.2 \text{ K})$, it is assumed that f_a for the particles is the same as that for the foils. Now the expression

$$\frac{S(\sigma_0 n f_a(T) F_a(T))}{S(\sigma_0 n f_a(4.2 \text{ K}) F_a(4.2 \text{ K}))} \tag{15}$$
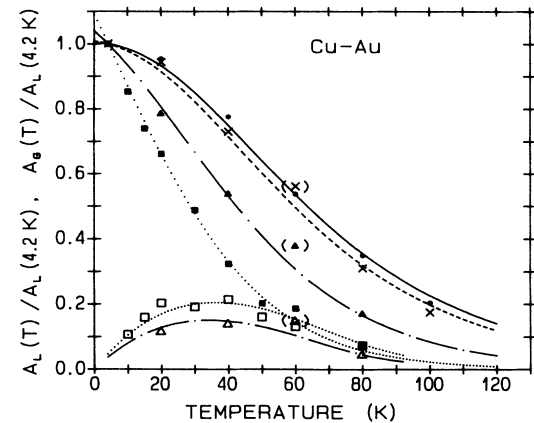

FIG. 5. Plot of the absorption area per unit background A_L of the Lorentzians determined by Lorentzian-plus-Gaussian fit and normalized to the value at 4.2 K as a function of temperature for Cu-Au samples of different packing fractions. ●, foil; X 54.3% sinter; ▲, 26.7% sinter; ■, powder. The absorption area per unit background A_G of the Gaussians normalized to $A_L(4.2 \text{ K})$ is also plotted vs temperature for two samples. △, 26.7% sinter; □, powder. For the foil and the 54.3% sinter, the Gaussian component was neglected in the fit. The curves for the Lorentzians represent the calculated results based on a dispersion theoretical model fitted to the plotted data, while curves for the Gaussians are polynomial fits to the data points. The data points in parentheses were neglected in the fittings.
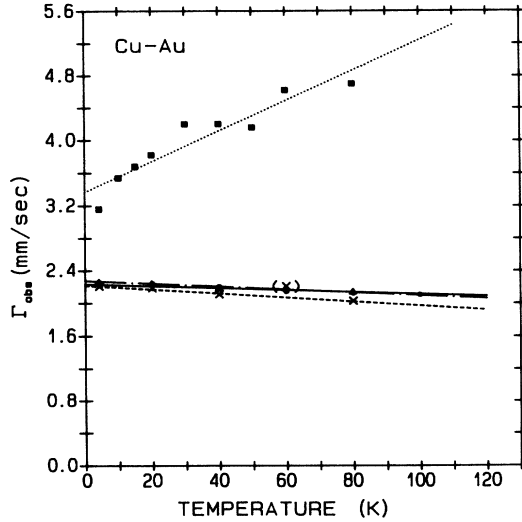
FIG. 6. Plot of the linewidth Γ_{obs} of the Lorentzians determined by Lorentzian-plus-Gaussian fit as a function of temperature for Cu-Au samples of different packing fractions. ●, foil; ×, 54.3% sinter; ▲, 26.7% sinter; ■, powder. For foil and the 54.3% sinter, the Gaussian component was neglected in the fit. The straight lines are the least-squares-fits to the data. The data point in parentheses was neglected in the fitting.
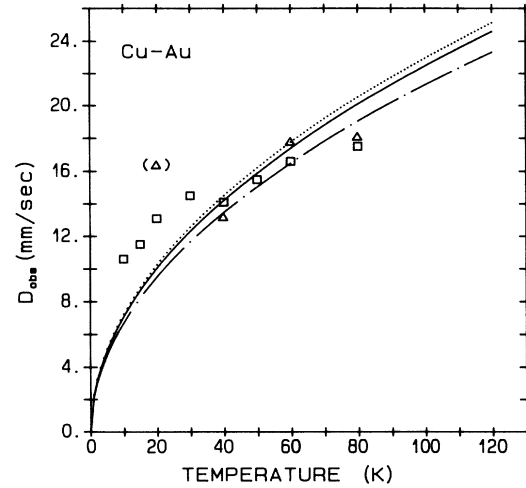

FIG. 7. Plot of the linewidth D_{obs} of the Gaussians determined by Lorentzian-plus-Gaussian fit as a function of temperature for two Cu-Au samples. △, 26.7% sinter; □, powder. The dashed-dotted and dotted curves are the results of model fitting. The data point in parentheses was neglected in the fitting. The solid line represents the theoretical curve, $2(\ln 2)^{1/2}\Delta$ vs temperature.

is to fit to the data of $A_L(T)/A_L(4.2$ K$)$. $F_a(T)$ is given by [see Eq. (9)]

$$F_a(T) = \exp(-2W_a^{PO})$$

$$= \exp\left[-P\int_0^\infty \frac{\Phi(z)}{z}\coth\left[\frac{z}{2k_BT}\right]dz\right] . \quad (16)$$

Assuming that the density of states $\Phi(z)$ for PO is a flat function such that

$$\Phi(z) = \begin{cases} \dfrac{1}{z_2-z_1} & \text{for } z_1 \leq z \leq z_2 \\ 0 & \text{otherwise,} \end{cases} \quad (17)$$

where $0 < z_1 < z_2$, there are two free parameters, z_1 and z_2, in the fit. The results are tabulated in Table II. The calculated curves $F_a(T)$ are shown in Fig. 8,

while the fitted curves of $A_L(T)/A_L(4.2$ K$)$ $[=S(\sigma_0 n f_a(T)F_a(T))/S(\sigma_0 n f_a(4.2$ K$)F_a(4.2$ K$))]$ are given by the dashed, dashed-dotted, and dotted lines in Figs. 2(b) and 5. It follows from these figures that the temperature dependence of A_L is satisfactorily explained by the present model.

Using the values of f_a and F_a obtained from the fits, the effective absorber thickness t_a has been calculated for each sample. Furthermore, the saturation-effect-corrected values of Γ_{obs} have been determined by the use of the saturation function for linewidth, which is also tabulated as a function of t_a by Trooster and Viegers.[16] Now, the corrected linewidths Γ_{obs} plotted versus T turned out to be nearly constant for all samples except for the Cu-Au powder one.

According to Fig. 6, the width Γ_{obs} of the Lorentzian line for the powder is substantially larger than those for the foil and the sinters at all temperatures and increases rapidly with temperature. This behavior of the powder sample is very different from those of the sinters and the

TABLE II. Debye temperature Θ for the Au impurity atoms in a Cu-3.60 at. % Au and Ag-3.33 at. % Au alloy, and the lower and upper limit z_1 and z_2 of the energy range of particle oscillation modes determined from Mössbauer measurements and their equivalent temperatures for Cu-Au and Ag-Au samples of different packing fractions.

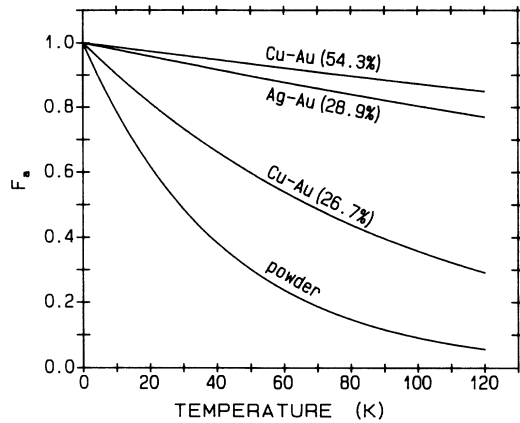| Sample	Θ (K)	z_1 (erg)	z_2 (erg)	z_1/k_B (mK)	z_2/k_B (mK)
Cu-Au foil					
54.3% Cu-Au sinter	206	16.7×10^{-19}	6.72×10^{-17}	12.1	487
26.7% Cu-Au sinter		5.51×10^{-19}	2.73×10^{-17}	3.99	198
Cu-Au powder		2.75×10^{-19}	2.53×10^{-17}	2.00	183
Ag-Au foil	167				
28.9% Ag-Au sinter		1.12×10^{-17}	1.42×10^{-16}	81.7	1030

FIG. 8. Temperature dependence of the calculated recoilless fraction F_a for Cu-Au and Ag-Au sinters of different packing fractions and a Cu-Au powder sample.

foils. The values of z_2 ($=z_{max}^{PO}$) in Table II assure that $z/2k_B T \ll 1$ in the whole range of temperature of the measurements. Hence it follows from Eq. (7) that

$$\Delta \approx 2(Pk_B T)^{1/2} . \tag{18}$$

The theoretical width of the PO band, $2(\ln 2)^{1/2}\Delta$, calculated using Eq. (18), is plotted versus T in Fig. 7. In the calculation, the diameter of the Cu-Au particles was assumed to be 150 nm. The width of the PO band is only determined by the recoil energy of a free particle, P (or the mass of the particle, M_0), and does not depend on the details of the frequency spectrum $\Phi(z)$, as long as the frequencies are sufficiently low. In actual samples, there will be a distribution of particles with respect to M_0, which will cause a distribution of Gaussians with respect to Δ. If the mass of some particles is much larger than $\langle M_0 \rangle$, the corresponding Gaussians will be so narrow that the latter could not be separated from the Lorentzian line. Then, it is expected that the Lorentzian line will effectively become broadened. Presence of such particles is unlikely in our samples, because the observed linewidths Γ_{obs} for the sinters are nearly equal to that for the foil. However, the very broad widths of the Lorentzian lines observed for the powder sample may be explained in the following way: In a system in which particles are loosely packed, there will be clusters of particles

and even clusters of clusters; this is a feature characteristic of fractal systems.[17] Then the system is of a three-grade structure consisting of atoms, particles, and clusters, and there must appear in the spectrum an absorption band due to the oscillation of the clusters in addition to the phonon wing and the PO band. The new band will be much narrower than the PO band and inseparable from the Lorentzian line, thus producing an effect similar to that of particles of very large mass. [Experimental data projecting beyond the peak of the fitted curves in Fig. 4(b) suggest the presence of narrow lines of natural width.] Hence the observed broad Lorentzian lines, the width of which increases with increasing temperature, can be interpreted as arising from cluster oscillations. Comparison between Γ_{obs} and D_{obs} of the powder sample (Figs. 6 and 7) indicates that the smallest effective clusters are of the size of about 20 particles.

It follows from Fig. 5 that, for Cu-Au, the normalized absorption area $A_L(T)/A_L(4.2$ K) decreases in the order foil $> 54.3\%$ sinter $> 26.7\%$ sinter $>$ powder at all temperatures, while $A_G(T)/A_L(4.2$ K) is always larger for the powder than for the 26.7% sinter. These results are quite reasonable. However, if the mass of the particles is sufficiently small causing very broad Gaussians, say for instance more than 20 times broader than the Lorentzian line, the Gaussians will merge in the background. This effect may partly account for the discrepancy between $A_L + A_G$ for the powder and A_L for the foil; according to Eq. (11), $A_L + A_G$ for the powder should be equal to A_L for the foil, whereas experimentally the former is much smaller than the latter. This discrepancy also exists between the sintered samples and the foil.

The assumption that $\Phi(z)$ is a flat function is based on the suggestion of Rutherford et al.[5] that the density of states for the localized modes is a constant over the whole frequency range of the modes; this has some theoretical grounds based on percolation and fractal models of disordered media.[18] According to the model of Rutherford et al.,[5] there is a discontinuity in density of states at the crossover frequency, below which the density of states for the continuous medium phonons is very low (Fig. 1 of Ref. 8). Thus $\Phi(z)$ may be assumed to consist only of the energy spectrum of the localized modes.

In Table III are tabulated v_1 and v_2, the calculated lower and upper limit of frequency range of the localized modes. The frequency v_1 is the crossover frequency between the continuous medium phonons and the localized

TABLE III. Lower and upper limit v_1 and v_2 of the frequency range of particle oscillation modes determined from ultrasonic and mechanical measurements and their equivalent energies and temperatures for Cu-Au and Ag-Au samples of different packing fractions.

Sample	v_1 (Hz)	v_2 (Hz)	hv_1 (erg)	hv_2 (erg)	hv_1/k_B (mK)	hv_2/k_B (mK)
54.3% Cu-Au sinter	8.0×10^8		5.3×10^{-18}		39	
26.7% Cu-Au sinter	2.0×10^8	2.4×10^{10}	13×10^{-19}	1.6×10^{-16}	9.6	1160
Cu-Au powder	0		0		0	
68.4% Ag-Au sinter	2.0×10^9	5.3×10^{10}	1.3×10^{-17}	3.5×10^{-16}	96	2500
28.9% Ag-Au sinter	4.0×10^8		2.7×10^{-18}		19	

modes, and v_2 is the low-frequency cutoff of the bulk pho-
nons in the particles, and these frequencies multiplied by
h are to be compared with the energy limits z_1 and z_2 of
the function $\Phi(z)$ [see Eq. (17)]. The calculation of v_1
and v_2 was carried out on the assumption that $\lambda_1 = 10d$
and $\lambda_2 = d$, in accordance with the postulation of Ruther-
ford et al.[5] λ_1 and λ_2 are the wavelengths of the phonons
at the crossover and at the low-frequency cutoff, respec-
tively, and d is the average diameter of the particles
(Table I). In the calculation, the continuous medium
phonon velocity is assumed to be 1200, 300, 1000, and
200 m/sec for the 54.3% Cu-Au, 26.7% Cu-Au, 68.4%
Ag-Au, and 28.9% Ag-Au sintered samples, respectively,
estimated from the ultrasonic and mechanical measure-
ments on 1-μm copper and silver sinters.[8] The bulk met-
al phonon velocities 3640 m/sec (Cu) and 2630 m/sec
(Ag) were adopted from the American Institute of Physics
Handbook.[19] It is supposed that no continuous medium
phonons exist in the powder sample of Cu-Au and hence
$v_1 = 0$, since the experimental results of Ref. 8 suggest
that a sample with such a low packing fraction is below
the percolation threshold. Comparison between Table II
and Table III shows that the lower and the upper limit,
z_1 and z_2, estimated from the present Mössbauer data as-
suming a flat energy spectrum, $\Phi(z)$, agree within a fac-
tor of 2–6 with the values hv_1 and hv_2 calculated on the
basis of the fracton model using the ultrasonic and
mechanical data for the sinters. For the Cu-Au powder
sample, z_1 equals k_B times 2.00 mK, while hv_1 is expect-
ed to be zero according to the fracton model.

It has been argued by Visscher[20] and also by Singwi
and Sjölander[15] that the shape of the phonon wing is re-
lated in a simple way to the energy spectrum $\phi_a(z)$, thus
$\phi_a(z)$ can at least in principle be determined from the
measurement of the phonon wing. However, such a mea-
surement is practically impossible as the wing extends at
least up to an energy of the order of $k_B\Theta$, where Θ is the
Debye temperature, and this energy range is too wide for
Mössbauer spectroscopy. Indeed, so far no Mössbauer
observations of phonon wings have been reported. But,
owing to the narrowness of their widths, the PO bands
could have been detected in the Mössbauer spectra.

Broad lines similar to the PO bands have been ob-
served for various systems in which the dynamics is con-
trolled by diffusive motions.[21–31] These are classified
into four categories: (1) molecular motions in super-
cooled liquids,[21] (2) dynamics of macromolecules in bio-
logical systems,[22–25] (3) localized diffusion in solids,[26–30]
and (4) diffusive motions of microcrystals.[31] Category (1)
is irrelevant to the present case. In view of the fact that
freeze-dried myoglobin exhibits no protein dynam-
ics,[23,32,33] mechanism (2) is also inconceivable for the
present systems of metallic microcrystals. Moreover, in
those biological systems, the peculiar changes take place
in a narrow temperature interval at fairly high tempera-
tures, suggesting the existence of a triggering mechanism
influenced by, for example, onset of water mobility.[22,23]
This is very different from the behavior of the present
systems.

The two Cu-Au sinters which have been measured

differ only in packing fraction, while there must be no
difference between them with respect to the internal
structure of individual particles because all particles have
been evaporated and sintered simultaneously in one and
the same vessel. And yet their Mössbauer spectra are
different. Therefore the broad components observed for
the 26.7% sinter are not caused by localized diffusion in
the particles. Although the powder sample has under-
gone no heat treatment after the evaporation, the fact
that the diffusion in cage is observed only for heavily
radiation-damaged crystals[26,27,29] suggests that the possi-
bility of (3) is very little also for the powder sample. Ac-
cording to previous studies,[34–36] neighboring particles in
the sinters are connected by neck (bridge) formation un-
der the present sintering condition. The scanning-
electron-microscopic observation of the sinter surfaces in-
dicates bridge connection between the particles, although
the resolution is not very good. Hence, as far as the
sinters are concerned, phononlike vibrations of the parti-
cles are very plausible while diffusive motions of the par-
ticles are unlikely.

Examination by scanning electron microscopy of a
small fraction of the Cu-Au powder sample dispersed on
a substrate has shown a bridge-connected network in
each cluster of particles. In the sample, however, most of
the contact points between the particles will have no
bridge. Therefore, for the powder sample, some kinds of
diffusive motion of the particles, such as diffusive tilting
motions proposed by Eynatten et al.,[31] are conceivable.
According to the model theories,[23–25,27–31] diffusive
motions of categories (1)–(4) cause a Mössbauer spec-
trum which can be approximated by a single broad
Lorentzian line or two Lorentzian lines, one narrow and
one broad. Two Lorentzians of different widths were
fitted to the experimental Mössbauer spectra of the Cu-
Au powder sample and the result showed that the fit was
as good as for the fittings of Fig. 4(b). Thus, for the
powder sample, the possibility of diffusive motions of par-
ticles cannot be excluded. To find out which model is
correct, very accurate experiments with well-
characterized samples will be necessary.

In the previous work,[13] no perceivable effect of PO on
Mössbauer effect was observed for the Ag-Au sinters.
This result was attributed to the largeness of the particle
size, 250 nm average diameter. (For the Cu-Au sinters
with an average diameter of 50 nm the effect was clearly
observed.) However, in the present study the effect is also
much less for the Ag-Au sinters than for the Cu-Au
sinters despite the fact that the average diameter for the
Ag-Au particles (50 nm) is much smaller than for the
Cu-Au particles (150 nm). Hence it can be concluded
that the difference between Cu and Ag must be attributed
to the fact that Ag particles will have much stronger ten-
dency to fuse together, i.e., they will be much more
strongly bound to each other, than Cu particles.

V. CONCLUSION

For sintered Cu and Ag small particles, which are
doped with Au impurities, a decrease in resonant absorp-
tion area of the Mössbauer spectrum is found compared

to the values found for bulk alloys. The lower the packing fraction of the particles, the larger is the observed decrease. In addition, in the spectra for a Cu-Au sinter of low packing fraction (26.7%), a broad spectral component was clearly observed, superimposed on the normal Mössbauer line as measured for the bulk alloys, and the former was interpreted to be PO band. These results provide experimental evidence for the existence of low-frequency modes arising from oscillations of the particles in the sinters. These low-frequency modes have been assumed without concrete experimental evidence to be the principal origin of the anomalous Kapitza resistance. The reduction in Mössbauer absorption area and the appearance of the broad component are more conspicuously demonstrated by a powder sample in which the small particles are loosely packed without sintering. The PO bands owe their detectability to the narrowness of the width, in contrast to the phonon wings, which have very wide widths.

The temperature dependence of the Mössbauer absorption area can satisfactorily be accounted for using a model based on the dispersion theory combined with the Debye model and the fracton model used for describing the energy spectra of the phonons and the PO, respectively. By using this model, and taking account of saturation effects, the recoilless fractions f_a and F_a can also be evaluated. The result shows that the value of f_a at 0 K is 0.253 for the Cu-Au foil and 0.184 for the Ag-Au foil, the corresponding Debye temperature being 206 and 167 K, respectively. The result also shows that F_a at 0 K is nearly equal to unity for all the sinters and the powder.

According to the fracton model applied to the sinters, the low-frequency modes are localized and have a flat energy spectrum extending over a clearly defined frequency range. The lower and the upper limit of the frequency range calculated on the basis of the fracton model using ultrasonic data on 1-μm copper and silver sinters coincide within a factor of 6 with the values estimated from the present Mössbauer results assuming a flat density of states for PO. Moreover, these frequency ranges include the frequencies which are most effective for the energy transfer in the millikelvin temperature range. This order-of-magnitude agreement provides further support for the existence of the low-frequency modes and for their localized nature as well.

The Mössbauer line observed for the powder sample is significantly broader than those for the sinters and the foils. This can be explained by the presence of very narrow PO bands which overlap the Mössbauer line and which cannot be separated from it. The narrow PO bands are ascribed to clustering of particles or even clustering of clusters. However, it is possible that the peculiar Mössbauer spectra are caused by some kind of diffusive motion of the particles in the powder sample, in which many particles must be contacting the others without bridge.

ACKNOWLEDGMENTS

*Permanent address: Physics Department, Toyama Medical and Pharmaceutical University, Toyama 930-01, Japan.

†Present address: Agrophysics Department, University of Agriculture Wageningen, Duivendaad 2, 6701 AP Wageningen, The Netherlands.

[1] O. Avenel, M. P. Berglund, R. G. Gylling, N. E. Phillips, A. Vetsleseter, and M. Vuorio, Phys. Rev. Lett. 31, 76 (1973).

[2] B. Frisken, F. Guillon, J. P. Harrison, and J. H. Page, J. Phys. (Paris) Colloq. 42, C6-858 (1981).

[3] N. Nishiguchi and T. Nakayama, Solid State Commun. 45, 877 (1983).

[4] A. I. Ahonen, M. P. Berglund, M. T. Haikala, M. Krusius, O. V. Lounasmaa, and M. A. Paalanen, Cryogenics 16, 521 (1976); K. Anders and W. O. Sprender, in Proceedings of the 14th International Conference on Low Temperature Physics edited by M. Krusins and M. Vuorio (North-Holland, Amsterdam, 1975), Vol. 1, p. 123.

[5] A. R. Rutherford, J. P. Harrison, and M. J. Stott, J. Low Temp. Phys. 55, 157 (1984).

[6] S. Alexander and R. Orbach, J. Phys. (Paris) Lett. 43, L625 (1982).

[7] S. Alexander, C. Laermans, R. Orbach, and H. M. Rosenberg, Phys. Rev. B 28, 4615 (1983).

[8] M. C. Maliepaard, J. H. Page, J. P. Harrison, and R. J. Stubbs, Phys. Rev. B 32, 6261 (1985).

[9] M. P. A. Viegers and J. M. Trooster, Phys. Rev. B 15, 72 (1977).

[10] G. von Eynatten and H. E. Bömmel, Appl. Phys. 14, 415 (1977); G. von Eynatten, J. Horst, K. Dransfeldt, and H. E. Bömmel, Hyp. Interactions 28, 1311 (1986).

[11] M. Hayashi, I. Tamura, Y. Fukano, and S. Kanemaki, Phys. Lett. 77A, 332 (1980).

[12] M. Hayashi, I. Tamura, Y. Fukano, and S. Kanemaki, Surf. Sci. 106, 456 (1981).

[13]M. Hayashi, I. Tamura, and H. Sakai, Jpn. J. Appl. Phys. 25, L905 (1986).

[14]L. van Hove, Phys. Rev. 95, 249 (1954).

[15]K. S. Singwi and A. Sjölander, Phys. Rev. 120, 1093 (1960).

[16]J. M. Trooster and M. P. A. Viegers, Möss. Effect. Data Ref. J. 1, 154 (1978).

[17]S. R. Forrest and T. A. Witten, J. Phys. A 12, L109 (1979); T. A. Witten and L. M. Sander, Phys. Rev. B 27, 5686 (1983); R. M. Brady and R. C. Ball, Nature (London) 309, 225 (1984); F. Argoul, A. Arneodo, G. Grasseau, and H. L. Swinney, Phys. Rev. Lett. 61, 2558 (1988).

[18]S. Alexander, J. Bernasconi, W. R. Schneider, and R. Orbach, Rev. Mod. Phys. 53, 175 (1981); C. J. Lambert, J. Low Temp. Phys. 59, 123 (1985); O. Entin-Wohlman, S. Alexander, R. Orbach, and K. W. Yu, Phys. Rev. B 29, 4588 (1984); S. Alexander and R. Orbach, Phys. Lett. 98A, 357 (1983).

[19]American Institute of Physics Handbook, 3rd ed., edited by D. E. Gray (McGraw-Hill, New York, 1972).

[20]W. M. Visscher, Ann. Phys. (N.Y.) 9, 194 (1960).

[21]D. C. Champeney and F. W. D. Woodhams, J. Phys. B 1, 620 (1968).

[22]H. Fraunfleder, G. A. Petsko, and D. Tsernoglou, Nature (London) 280, 558 (1979).

[23]F. Parak, E. W. Knapp, and D. Kucheida, J. Mol. Biol. 161, 177 (1982).

[24]E. W. Knapp, S. F. Fischer, and F. Parak, J. Chem. Phys. 78, 4701 (1983).

[25]I. Nowik, E. R. Bauminger, S. G. Cohen, and S. Ofer, Phys. Rev. A 31, 2291 (1985).

[26]G. Vogl, W. Mansel, and P. H. Dederichs, Phys. Rev. Lett. 36, 1497 (1976).

[27]W. Petry, G. Vogl, and W. Mansel, Phys. Rev. Lett. 45, 1862 (1980).

[28]W. Petry and G. Vogl, Z. Phys. B 45, 207 (1982).

[29]W. Petry, G. Vogl, and W. Mansel, Z. Phys. B 46, 319 (1982).

[30]R. Wordel, F. J. Litterst, and F. E. Wagner, J. Phys. F 15, 2525 (1985).

[31]G. von Eynatten, T. Ritter, H. E. Bömmel, and K. Dransfeld, Z. Phys. B 65, 341 (1987).

[32]F. Parak and H. Formanek, Acta Crystallogr. Sect. A 27, 253 (1971).

[33]Yu. Krupjanskii, F. Parak, V. I. Goldanskii, R. L. Mössbauer, E. E. Gaubmann, H. Engelmann, and I. P. Suzdalev, Z. Naturforsch. 37C, 57 (1982).

[34]W. D. Kingery and M. Berg, J. Appl. Phys. 26, 1205 (1955).

[35]S. Iwama and K. Hayakawa, Jpn. J. Appl. Phys. 20, 335 (1981).

[36]K. Rogacki, M. Kubota, E. G. Syskakis, R. M. Meuller, and F. Pobell, J. Low Temp. Phys. 59, 397 (1985).